Check for updates

CHEMISTRY
A European Journal

A Journal of
ChemPubSoc Europe

Accepted Article

Title: A peri-Xanthenoxanthene Centered Columnar-Stacking Organic Semiconductor for High-Efficiency, Photothermal Stable Perovskite Solar Cells

Authors: Niansheng Xu, Yang Li, Ruihan Wu, Rui Zhu, Jidong Zhang, Shaik Zakeeruddin, Hangying Li, Ze-Sheng Li, Michael Graetzel, and Peng Wang

This manuscript has been accepted after peer review and appears as an Accepted Article online prior to editing, proofing, and formal publication of the final Version of Record (VoR). This work is currently citable by using the Digital Object Identifier (DOI) given below. The VoR will be published online in Early View as soon as possible and may be different to this Accepted Article as a result of editing. Readers should obtain the VoR from the journal website shown below when it is published to ensure accuracy of information. The authors are responsible for the content of this Accepted Article.

To be cited as: *Chem. Eur. J.* 10.1002/chem.201806015

Link to VoR: http://dx.doi.org/10.1002/chem.201806015

Supported by
ACES

WILEY-VCH

10.1002/chem.201806015

WILEY-VCH

COMMUNICATION

A *peri*-Xanthenoxanthene Centered Columnar-Stacking Organic Semiconductor for High-Efficiency, Photothermal Stable Perovskite Solar Cells

Niansheng Xu, Yang Li, Ruihan Wu, Rui Zhu, Jidong Zhang, Shaik M. Zakeeruddin, Hanying Li, Ze-Sheng Li, Michael Grätzel and Peng Wang*

Abstract: Modulating the structure and property of hole-transporting organic semiconductors is of paramount importance for high-efficiency and stable perovskite solar cells (PSCs). Herein we report a low-cost *peri*-xanthenoxanthene based small-molecule P1, which is prepared at a total yield of 82% via a three-step synthetic route from the low cost starting material 2-naphthol. P1 molecules stack in one-dimensional columnar arrangement characteristic of strong intermolecular π–π interactions, contributing to the formation of a solution-processed, semicrystalline thin-film exhibiting one order of magnitude higher hole mobility than the amorphous one based on the state-of-the art hole-transporter, 2,2-7,7-tetrakis(*N*,*N*′-di-paramethoxy-phenylamine 9,9′-spirobifluorene (spiro-OMeTAD). PSCs employing P1 as the hole-transporting layer attain a high efficiency of 19.8% at the standard AM1.5G conditions, and good long-term stability under continuous full sunlight soaking at 40 °C.

Organic–inorganic halide PSCs have attracted great attention owing to inexpensive precursors for photoactive layer, energy-saving fabrication protocols, and high power conversion efficiencies (PCEs).[1] Improving the long-term operational stability is crucial for future practical application of PSCs.[2] In a typical PSC, a hole-transporting layer is indispensable affording selective hole-extraction from the photo-excited perovskite and their transportation to the positive electrode. In this context, a lot of organic semiconductors have been explored,[3,4] among which the state-of-the-art spiro-OMeTAD is very efficient. For large-scale application, spiro-OMeTAD is however limited by high preparation and purification cost, low hole mobility, and severe degradation of photovoltaic performance under a thermal stress.[5] So far only a few hole-transporting candidates can achieve comparable photovoltaic performance to spiro-OMeTAD, with PCEs close to or exceeding 20%.[1k,4f,4i,4j,6] On the other hand, unlike inorganic[7] and polymeric hole-transporting materials,[8] small-molecule based hole-transporters are scarcely reported for stable perovskite solar cells under thermal and light dual stress.[9] In 2018, Shang and his co-workers[10] utilized a benzodipyrrole-based hole-conductor for a 17.2%-efficiency PSC exhibiting good stability at 35 °C. Later, Lee et al.[1k] reported a fluorene-terminated hole-conductor for a 60 °C stable PSC stored in the dark.

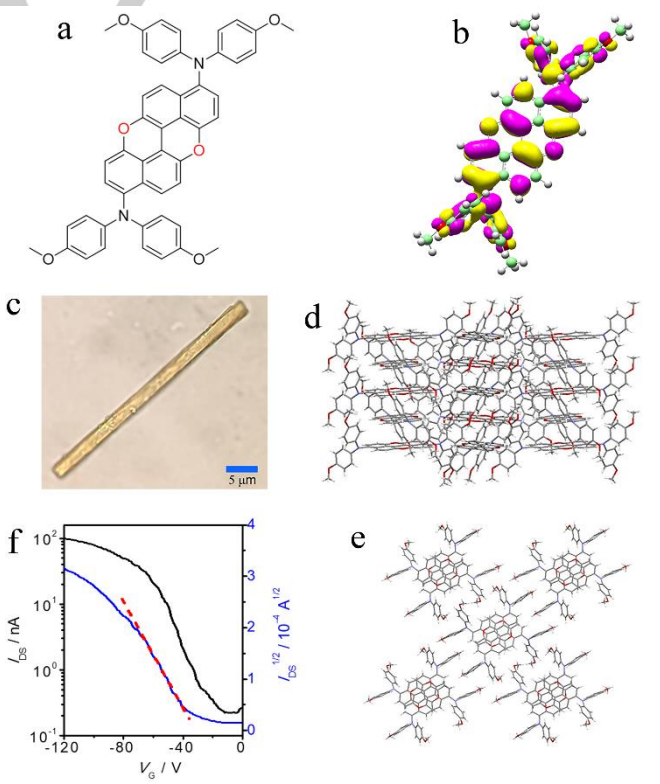

Figure 1. (a) Chemical structure of P1, (b) HOMO distribution, and (c) single-crystal optical microscopy image of P1. Crystal structures along (d) *a* axis view and (e) *b* axis view. (f) Transfer characteristic of single-crystal field-effect transistor (V_{DS} = –120 V).

Our strategy for high-performance small-molecule based hole-conductors in PSCs consists in the functionalization of a planar π-conjugated two-dimensional heterocycle with multiple electron-donating bisarylamino substituents to fine-tune its orbital energy,

[a] N. Xu, Prof. P. Wang
Center for Chemistry of Novel & High-Performance Materials
Department of Chemistry
Zhejiang University
Hangzhou 310028, China
[b] Y. Li, Dr. S. M. Zakeeruddin, Prof. M. Grätzel
Laboratory of Photonics and Interfaces
Institute of Chemical Sciences & Engineering
École Polytechnique Fédérale de Lausanne
CH-1015 Lausanne, Switzerland
[c] Y. Li, Prof. J. Zhang
Changchun Institute of Applied Chemistry
Chinese Academy of Sciences, Changchun 13002, China
[d] R. Wu, Prof. H. Li
Department of Polymer Science and Engineering
Zhejiang University
Hangzhou 310027, China
[e] R. Zhu, Prof. Z Li
School of Chemistry
Beijing Institute of Technology
Beijing 10081, China

Supporting information for this article is given via a link at the end of the document.((Please delete this text if not appropriate))

Accepted Manuscript

This article is protected by copyright. All rights reserved.

10.1002/chem.201806015

and significantly enhance hole mobility via core-to-core stacking. As a model example, we design a *peri*-xanthenoxanthene[11] (PXX) centered small-molecule, N^3,N^3,N^9,N^9-tetrakis(4-methoxyphenyl)xantheno[2,1,9,8-*klmna*]xanthene-3,9-diamine (abbreviated as P1, Figure 1a), for high-performance PSCs.

The synthesis of P1 was carried out in a total yield of 82%, via three-steps of aerobic C−H/C−O cyclization,[12] bromination, and Buchwald-Hartwig cross-coupling from low-cost 2-naphthol (Scheme S1). Note that the overall cost of materials for 1 gram of P1 in our lab (Table S1) is estimated to be less than one tenth of that for spiro-OMeTAD.[5j] In addition, only one-time column purification is required during the whole synthetic process, making large-scale synthesis and application viable. Density functional theory (DFT) calculations reveal that the highest occupied molecular orbital (HOMO) energy level of P1 is –4.57 eV in vacuum, which is slightly deeper than that of spiro-OMeTAD (–4.49 eV). As depicted in Figure 1b, the HOMO of P1 is delocalized over the whole π-conjugated skeleton, which is crucial for intermolecular hole-hopping. Thermogravimetric analysis (TGA) shows that P1 exhibits excellent thermal stability, with a >370 °C decomposition temperature (Figure S1).

To fully elucidate the molecular packing and charge-transport characteristics of P1 in solid state, we grew its single-crystals by slowly evaporating a saturated methanol/dichloromethane solution. The as-grown P1 single-crystals present an overall crack-free morphology and distinct borders (Figure 1c). X-ray crystallographic structure analysis shows that it forms one-dimensional π-stacked columnar motif along the *b* axis with an interplanar distance of 3.71 Å (Figure 1d,e, Figure S2, Table S2).[13] Each layer is further stapled in a staggered fashion. One column links to adjacent columns with multiple C-H/π and C-H/O interactions to form a three-dimensional network. To determine the hole mobility for the P1 single-crystal, a bottom-gate/top-contact single-crystal field-effect transistor was fabricated. The transfer curve (Figure 1f) display typical hole transport characteristics and an impressive hole mobility of ~2.59×10^{-3} cm^2 V^{-1} s^{-1}. Theoretical calculations were further performed based on the experimental single-crystal structure to gain deeper insight into the charge transport characteristics. The hole mobility of P1 was theoretically calculated by using the Einstein relation $\mu = eD/k_BT$ based on the hopping model.[14] With a large charge transfer integral along the axis of the column (~26 meV), the calculated mobility can reach up to 1.79×10^{-2} cm^2 V^{-1} s^{-1} (Figure S3 and Table S3).

We further executed space-charge-limited current measurements with a P1 thin film spun from chlorobenzene with a hole-only device. The average hole mobility of dopant-free P1 is 5.73×10^{-5} cm^2 V^{-1} s^{-1} (Figure S4), over 10 times higher than that of non-doped spiro-MeOTAD (4.95×10^{-6} cm^2 V^{-1} s^{-1}). Grazing-incidence wide-angle X-ray scattering (GIWAXS) of the P1 thin film was measured to probe the mesoscale molecular ordering, which is vital to the charge transport property. Figure 2a reveals the semicrystalline nature of spin-coated P1 film. The isotropic diffraction ring at 17 nm^{-1}, is related to a *d*-spacing of 0.37 nm, which is well consistent with the π-stacking reflection (0, 2, 0) from the single-crystal data (Table S2). In view of the amorphous feature of a spin-coated spiro-OMeTAD thin film (Figure S5),[15] the observed π-stacking ordering of the P1 thin film explains its much higher hole mobility. With lithium bis(trifluoromethylsulfonyl)imide and 4-*tert*-butylpyridine as additive, the hole mobility of P1 film was improved to 8.55 × 10^{-4} cm^2 V^{-1} s^{-1} (Figure S4), which is around four times higher than that of doped spiro-OMeTAD (1.89 × 10^{-4} cm^2 V^{-1} s^{-1}).

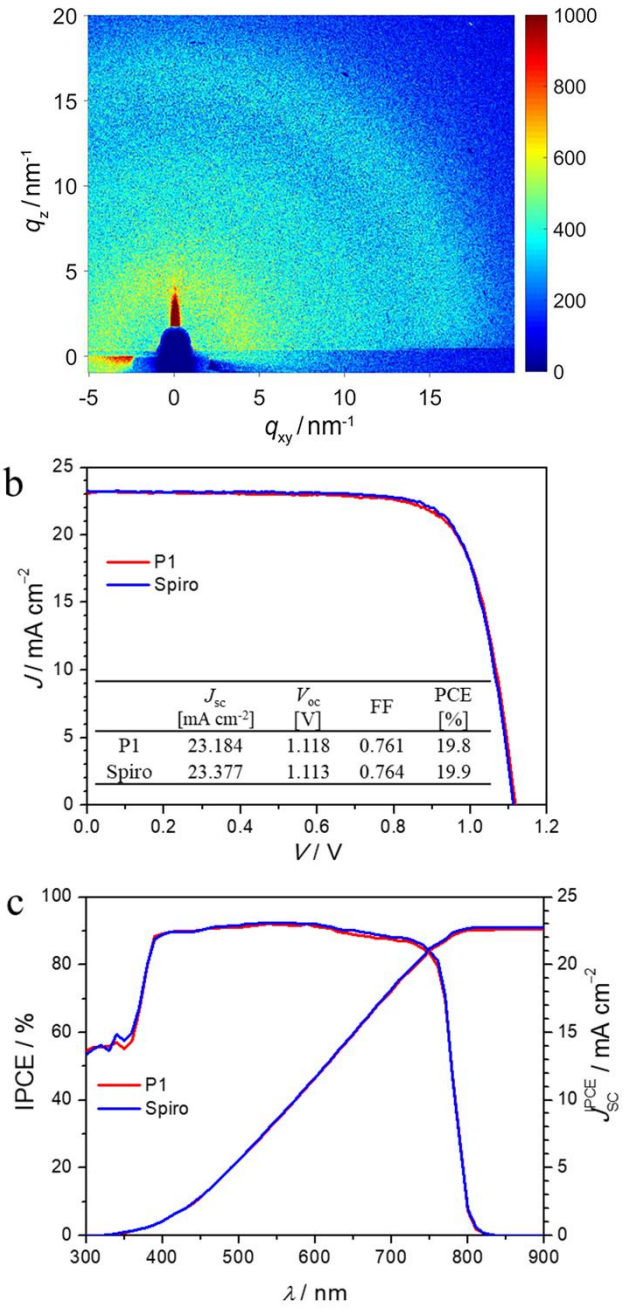

Figure 2. (a) GIWAXS maps for spin-coated thin films of P1. (b) *J*–*V* characteristic of a typical PSC with P1 measured under AM 1.5G illumination. The data for a control cell with spiro-OMeTAD is also included. (c) IPCE spectra and integrated J_{sc} from the IPCE curves.

To gain insight into the ability of P1 to extract holes from a perovskite layer, we carried out steady-state photoluminescence

Accepted Manuscript

This article is protected by copyright. All rights reserved.

10.1002/chem.201806015

(PL) and time-resolved photoluminescence (TRPL) measurements. Compared with a bare perovskite film ($Cs_{0.05}(FA_{0.83}MA_{0.17})_{0.95}Pb_{1.03}Br_{0.48}I_{2.52}$, abbreviated as Cs_5M),[16] the PL intensity of a P1-coated perovskite film is significantly attenuated (Figure S6a). The PL quenching yield with P1 is 98.0%, almost the same as the sample with spiro-OMeTAD (97.8%). As shown in Figure S6b, the bare perovskite film presents a long PL lifetime of ~243 ns. Once coated with organic semiconductors PL lifetimes decrease greatly, being 29.7 ns for the P1 sample and 40.6 ns for the spiro-OMeTAD sample. Note that the HOMO energy level of P1 derived from ultraviolet photoelectron spectroscopy measurement (Figure S7) is –5.25 eV, lower than that of spiro-OMeTAD (–5.13 eV). Interestingly, the hole extraction kinetics and yield do not decrease even with reduced hole extraction driving force.

We then used doped P1 as the hole-transporting layer to fabricate PSCs with Cs_5M as light-absorber. The details for cell fabrication are described in the Supporting Information. From atomic force microscopy (Figure S8a) and scanning electron microscopy (Figure S8c) images, some pinholes were observed for the doped P1 film on the perovskite layer. We optimized the thickness of hole-transporting layer in PSCs by use of 40, 50, 60, or 70 mM P1 in chlorobenzene. The photovoltaic parameters were shown in Figure S9 and Table S4. In average, the cells fabricated with 50 mM P1 presents the highest J_{sc} and FF, leading to a champion PCE. The *J-V* curves and incident-photon-to-collected-electron conversion efficiency (IPCE) spectra of the best-performed devices based on P1 and spiro-OMeTAD are shown in Figure 2b and 2c, respectively. The device with P1 has a J_{sc} of 23.184 mA cm^{-2}, a V_{oc} of 1118 mV, and an FF of 76.1%, generating a high PCE of 19.8%, which is comparable to the control cell with spiro-OMeTAD. Furthermore, the maximum power point tracking under AM 1.5G illumination (Figure S10) was conducted to eliminate the scan rate dependent device performance, and we got the stabilized PCE of 19.3% and 19.5% for P1 and spiro-OMeTAD based devices, respectively, which are similar with the results derived from the *J-V* curves. The integrated photocurrent densities calculated from the IPCE spectra of devices (Figure 2c) agreed closely with those obtained from the *J-V* curves, indicating that the spectrum of our simulator matches well with AM-1.5 standard solar radiation. The distributions of the photovoltaic parameters obtained from three batches were shown in Figure S11 and Table S5, which indicates the good reproducibility of the P1 based perovskite solar cells.

Photostability of PSCs (not encapsulated) was first evaluated with maximum power point (MPP) tracking under continuous light irradiation at ambient temperature in a nitrogen atmosphere. Figure 3a shows that the P1 based cell retained >95% of its initial efficiency after 300 h, better than the spiro-OMeTAD control. Further, we investigated the cell stability under the thermal and light dual stress (Figure 3b). After 1000 h continuous one sun illumination at 40 ºC, the P1 cell retained over 80% of its initial efficiency, which is much higher than that of 17% for the spiro-OMeTAD control. The enhanced operational stability of P1 based cell probably results from the improved T_g (Figure 3d), giving an indication for further design of organic semiconductors for PSCs.

Moisture induced decomposition of the perovskite layer is the critical degradation path[2a,17] in PSCs. Therefore, the hydrophobicity of the hole-transporting layer is also vital to the long-term stability towards environmental factors. We tested the hydrophobicity of P1 through measuring the contact angle formed by a thin film with a water droplet. The decreased wettability of the water droplet on the doped P1 based thin film compared to the doped spiro-OMeTAD film is apparent from Figures 3e and 3f which illustrate that the contact angle increases from 78.7 ° for the spiro-OMeTAD film to 92.2 ° for P1. We also monitored the cell stability in ambient atmosphere (Figure 3c and S12). The un-encapsulated device employing P1 retained 95% of the initial efficiency after 1000 h. In contrast, the spiro-OMeTAD control device showed only 80% retention. In addition, the photovoltaic performance remained almost unaltered in argon filled box (Figure S13 and Table S6) for both devices, confirming that moisture induced the degradation of the perovskite solar cell. The increased V_{oc} after 60 days could be related to the enlargement of perovskite grains triggered by spontaneous crystal coalescence.[18]

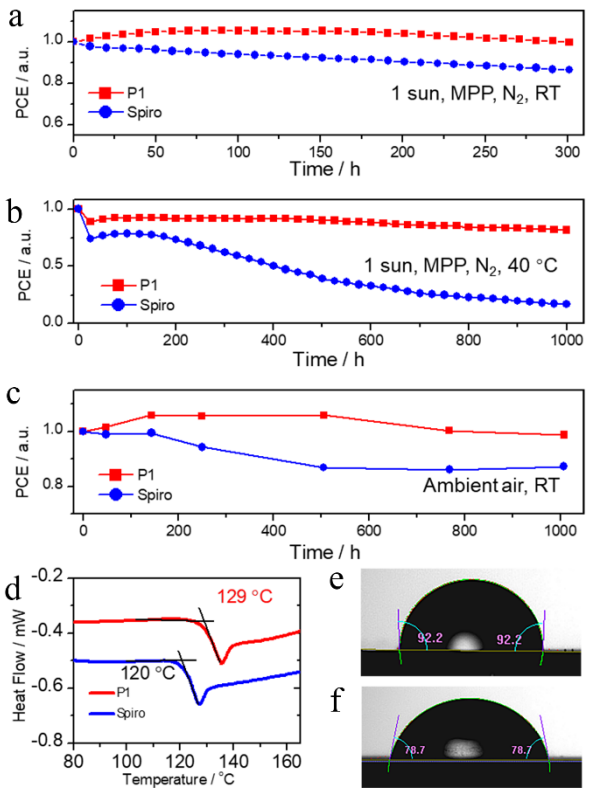

Figure 3. Evolution of normalized PCEs of un-encapsulated devices examined at MPP tracking under continuous light irradiation (AM 1.5 G, 100 mW cm^{-2}) at (a) room temperature and (b) 40 ºC under nitrogen. (c) Stability of un-encapsulated devices in air (humidity: 20–40%) under indoor light and room temperature. (d) Differential scanning calorimeter curves. Contact angle images of water on doped (e) P1 and (f) spiro-OMeTAD films.

To summarize, we have synthesized a *peri*-xanthenoxanthene -centered small-molecule as a remarkably cheap organic semiconductor for efficient and stable perovskite solar cells. The improved glass transition temperature and hydrophobicity of the

Accepted Manuscript

This article is protected by copyright. All rights reserved.

hole-transporting layer jointly contributed to the enhanced long-term device stability. The planar discotic conjugated backbone enables the formation of a one-dimensional columnar stacking via intermolecular π-π interactions, contributing to the high hole mobility of solution-processed thin films.

Acknowledgements ((optional))

N.X. and Y.L. contributed equally to this work. P.W. express sincere gratitude to the National 973 Program (2015CB932204), the National Science Foundation of China (No. 51673165 and No. 91733302), the Key Technology R&D Program (BE2014147-1) of Science and Technology Department of Jiangsu Province, and the Fundamental Research Fund (No.2017FZA3007) for the Central Universities for financial support. We thank beamline BL14B1 (Shanghai Synchrotron Radiation Facility) for providing the beam time during GIWAXS experiments.

Keywords: polycycles • organic semiconductor • charge transport • solar cell • photostability

[1] a) A. Kojima, K. Teshima, Y. Shirai, T. Miyasaka, *J. Am. Chem. Soc.* **2009**, *131*, 6050; b) H.-S. Kim, C.-R. Lee, J.-H. Im, K.-B. Lee, T. Moehl, A. Marchioro, S.-J. Moon, R. Humphry-Baker, J.-H. Yum, J. E. Moser, M. Graetzel, N.-G. Park, *Sci. Rep.* **2012**, *2*, 591; c) J. Burschka, N. Pellet, S.-J. Moon, R. Humphry-Baker, P. Gao, M. K. Nazeeruddin, M. Grätzel, *Nature* **2013**, *499*, 316; d) M. Liu, M. B. Johnston, H. J. Snaith, *Nature* **2013**, *501*, 395; e) G. Xing, N. Mathews, S. Sun, S. S. Lim, Y. M. Lam, M. Grätzel, S. Mhaisalkar, T. C. Sum, *Science* **2013**, *342*, 344; f) H. Zhou, Q. Chen, G. Li, S. Luo, T.-b. Song, H.-S. Duan, Z. Hong, J. You, Y. Liu, Y. Yang, *Science* **2014**, *345*, 542; g) W. Chen, Y. Wu, Y. Yue, J. Liu, W. Zhang, X. Yang, H. Chen, E. Bi, I. Ashraful, M. Grätzel, L. Han, *Science* **2015**, *350*, 944; h) N. J. Jeon, J. H. Noh, W. S. Yang, Y. C. Kim, S. Ryu, J. Seo, S. I. Seok, *Nature* **2015**, *517*, 476; i) D. Luo, W. Yang, Z. Wang, A. Sadhanala, Q. Hu, R. Su, R. Shivanna, G. F. Trindade, J. F. Watts, Z. Xu, T. Liu, K. Chen, F. Ye, P. Wu, L. Zhao, J. Wu, Y. Tu, Y. Zhang, X. Yang, W. Zhang, R. H. Friend, Q. Gong, H. J. Snaith, R. Zhu, *Science* **2018**, *360*, 1442; j) Best Research-Cell Efficiencies (NREL, 2018), https://www.nrel.gov/pv/assets/pdfs/pv-efficiencies-07-17-2018.pdf; k) N. J. Jeon, H. Na, E. H. Jung, T.-Y. Yang, Y. G. Lee, G. Kim, H.-W. Shin, S. I. Seok, J. Lee, J. Seo, *Nat. Energy* **2018**, *3*, 682.

[2] a) K. Domanski, E. A. Alharbi, A. Hagfeldt, M. Grätzel, W. Tress, *Nat. Energy* **2018**, *3*, 61; b) H. J. Snaith, P. Hacke, *Nat. Energy* **2018**, *3*, 459.

[3] a) L. Calió, S. Kazim, M. Grätzel, S. Ahmad, *Angew. Chem. Int. Ed.* **2016**, *55*, 14522; *Angew. Chem.* **2016**, *128*, 14740; b) J. Wang, K. Liu, L. Ma, X. Zhan, *Chem. Rev.* **2016**, *116*, 14675.

[4] a) N. J. Jeon, H. G. Lee, Y. C. Kim, J. Seo, J. H. Noh, J. Lee, S. I. Seok, *J. Am. Chem. Soc.* **2014**, *136*, 7837; b) H. Li, K. Fu, A. Hagfeldt, M. Grätzel, S. G. Mhaisalkar, A. C. Grimsdale, *Angew. Chem. Int. Ed.* **2014**, *53*, 4085; *Angew. Chem.* **2014**, *126*, 4169; c) J. Liu, Y. Wu, C. Qin, X. Yang, T. Yasuda, A. Islam, K. Zhang, W. Peng, W. Chen, L. Han, *Energy Environ. Sci.* **2014**, *7*, 2963; d) L. Zheng, Y.-H. Chung, Y. Ma, L. Zhang, L. Xiao, Z. Chen, S. Wang, B. Qu, Q. Gong, *Chem. Commun.* **2014**, *50*, 11196; e) K. Rakstys, A. Abate, M. I. Dar, P. Gao, V. Jankauskas, G. Jacopin, E. Kamarauskas, S. Kazim, S. Ahmad, M.Grätzel, M. K. Nazeeruddin, *J. Am. Chem. Soc.* **2015**, *137*, 16172; f) M. Saliba, S. Orlandi, T. Matsui, S. Aghazada, M. Cavazzini, J.-P. Correa-Baena, P. Gao, R. Scopelliti, E. Mosconi, K.-H. Dahmen, F. De Angelis, A. Abate, A. Hagfeldt, G. Pozzi, M. Graetzel, M. K. Nazeeruddin, *Nat. Energy* **2016**, *1*, 15017; g) B. Xu, D. Bi, Y. Hua, P. Liu, M. Cheng, M. Grätzel, L. Kloo, A. Hagfeldt, L. Sun, *Energy Environ. Sci.* **2016**, *9*, 873; h) I. Cho, N. J. Jeon, O. K. Kwon, D. W. Kim, E. H. Jung, J. H. Noh, J. Seo, S. I. Seok, S. Y. Park, *Chem. Sci.* **2017**, *8*, 734; i) F. Zhang, Z. Wang, H. Zhu, N. Pellet, J. Luo, C. Yi, X. Liu, H. Liu, S. Wang, X. Li, Y. Xiao, S. M. Zakeeruddin, D. Bi, M. Grätzel, *Nano Energy* **2017**, *41*, 469; j) Q.-Q. Ge, J.-Y. Shao, J. Ding, L.-Y. Deng, W.-K. Zhou, Y.-X. Chen, J.-Y. Ma, L.-J. Wan, J. Yao, J.-S. Hu, Y.-W. Zhong, *Angew. Chem. Int. Ed.* **2018**, *57*, 10959; *Angew. Chem.* **2018**, *130*, 11125.

[5] X. Zhao, H.-S. Kim, J.-Y. Seo, N.-G. Park, *ACS Appl. Mater. Interfaces* **2017**, *9*, 7148.

[6] a) B. Xu, J. Zhang, Y. Hua, P. Liu, L. Wang, C. Ruan, Y. Li, G. Boschloo, E. M. J. Johansson, L. Kloo, A. Hagfeldt, A. K. Y. Jen, L. Sun, *Chem* **2017**, *2*, 676; b) J. Zhang, B. Xu, L. Yang, A. Mingorance, C. Ruan, Y. Hua, L. Wang, N. Vlachopoulos, M. Lira-Cantú, G. Boschloo, A. Hagfeldt, L. Sun, E. M. J. Johansson, *Adv. Energy Mater.* **2017**, *7*, 1602736.

[7] a) W. Chen, Y. Wu, Y. Yue, J. Liu, W. Zhang, X. Yang, H. Chen, E. Bi, I. Ashraful, M. Grätzel, L. Han, *Science* **2015**, *350*, 944; b) N. Arora, M. I. Dar, A. Hinderhofer, N. Pellet, F. Schreiber, S. M. Zakeeruddin, M. Grätzel, *Science* **2017**, *358*, 768.

[8] M. Saliba, T. Matsui, K. Domanski, J.-Y. Seo, A. Ummadisingu, S. M. Zakeeruddin, J.-P. Correa-Baena, W. R. Tress, A. Abate, A. Hagfeldt, M. Grätzel, *Science* **2016**, *354*, 206.

[9] Q. Fu, X. Tang, B. Huang, T. Hu, L. Tan, L. Chen, Y. Chen, *Adv. Sci.* **2018**, *5*, 1700387.

[10] R. Shang, Z. Zhou, H. Nishioka, H. Halim, S. Furukawa, I. Takei, N. Ninomiya, E. Nakamura, *J. Am. Chem. Soc.* **2018**, *140*, 5018.

[11] S. Doi, A. Fujita, S. Ikeura, T. Inabe, Y. Matsunaga, *Bull. Chem. Soc. Jpn.* **1979**, *52*, 2494.

[12] T. Kamei, M. Uryu, T. Shimada, *Org. Lett.* **2017**, *19*, 2714.

[13] CCDC 1860987 contains the supplementary crystallo-graphic data for this paper. These data can be obtained free of charge from The Cambridge Crystallographic Data Centre.

[14] H. Qiu, T. Xu, Z. Wang, W. Ren, H. Nan, Z. Ni, Q. Chen, S. Yuan, F. Miao, F. Song, G. Long, Y. Shi, L. Sun, J. Wang, X. Wang, *Nat. Commun.* **2013**, *4*, 2642.

[15] U. Bach, D. Lupo, P. Comte, J. E. Moser, F. Weissörtel, J. Salbeck, H. Spreitzer, M. Grätzel, *Nature* **1998**, *395*, 583.

[16] a) M. Saliba, T. Matsui, J.-Y. Seo, K. Domanski, J.-P. Correa-Baena, M. K. Nazeeruddin, S. M. Zakeeruddin, W. Tress, A. Abate, A. Hagfeldt, M. Grätzel, *Energy Environ. Sci.* **2016**, *9*, 1989; b) H. Tan, A. Jain, O. Voznyy, X. Lan, F. P. García de Arquer, J. Z. Fan, R. Quintero-Bermudez, M. Yuan, B. Zhang, Y. Zhao, F. Fan, P. Li, L. N. Quan, Y. Zhao, Z.-H. Lu, Z. Yang, S. Hoogland, E. H. Sargent, *Science* **2017**, *355*, 722.

[17] J. Yang, B. D. Siempelkamp, D. Liu, T. L. Kelly, *ACS Nano* **2015**, *9*, 1955.

[18] B. Roose, A. Ummadisingu, J.-P. Correa-Baena, M. Saliba, A. Hagfeldt, M. Graetzel, U. Steiner, A. Abate, *Nano Energy* **2017**, *39*, 24.

Accepted Manuscript

This article is protected by copyright. All rights reserved.

10.1002/chem.201806015

WILEY-VCH

COMMUNICATION

Easy, high-efficiency and stable: A low-cost *peri*-xanthenoxanthene-centred columnar-stacking organic semiconductor has been prepared and used as hole-transporter in perovskite solar cells achieving a power conversion efficiency of 19.8 % and good long-term stability under continuous full sunlight soaking at 40 °C.

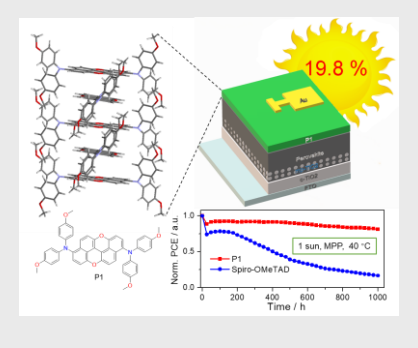

*Niansheng Xu, Yang Li, Ruihan Wu, Rui Zhu, Jidong Zhang, Shaik M. Zakeeruddin, Hanying Li, Ze-Sheng Li, Michael Grätzel and Peng Wang**

Page No. – Page No.

A *peri*-Xanthenoxanthene Centered Columnar-Stacking Organic Semiconductor for High-Efficiency, Photothermal Stable Perovskite Solar Cells

WILEY-VCH Accepted Manuscript

This article is protected by copyright. All rights reserved.